IMAGE ENHANCEMENT OF DATA SETS IN FLUORESCENT CONFOCAL MICROSCOPY

M. Čapek* **, L. Kubínová**, K. Hána* and P. Smrčka*

* Czech Technical University/Faculty of Biomedical Engineering, nám. Sítná 3105, 272 01 Kladno 2, Czech Republic
** Academy of Sciences of the Czech Republic/Institute of Physiology, Vídeňská 1083, 142 20 Prague 4, Czech Republic

capek@biomed.cas.cz

Abstract: A confocal laser scanning microscope (CLSM) is a non-invasive tool that gives possibility to obtain a series of fluorescent optical sections representing an investigated biological specimen through optical sectioning of 2D confocal planes. However, images captured from deep layers of the specimen may be darker than images from the topmost layers due to light aberrations and photobleaching. This effect causes difficulties in subsequent analysis of biological objects. We solved this problem by applying both an online method – a feedback-based tuning of the CLSM hardware during scanning, and an offline method – a histogram-warping-based algorithm. The methods were tested on real confocal image data captured from a rat skeletal muscle specimen. It was shown that both approaches diminish the light attenuation of images in the series.

Introduction

A confocal laser scanning microscope (CLSM) is a non-invasive tool that gives possibility to obtain a series of fluorescent optical sections, i.e. a 3D volume, representing a biological specimen through optical sectioning and scanning of 2D confocal planes [1]. However, fluorescent image intensities from a CLSM suffer from light loss distortions that can be described by two main effects – light aberrations and photobleaching.

Photobleaching means the irreversible destruction of fluorescence within a stained specimen. The effect of photobleaching can be partially reduced by adding antioxidants to the biological specimen or by decreasing the laser light intensity and by choosing the image exposure time smaller than the characteristic time on which bleaching of the fluorophore in the specimen occurs. Also it is difficult to stain a thick specimen by fluorophores evenly. Thus the amount of fluorophores may vary with depth of a specimen causing the light intensity attenuation.

Light aberrations include chromatic and spherical aberrations introduced by the optical elements in the microscope, refractive-index mismatch between the objective and the specimen, and aberrations resulting from focusing and light propagation through a turbid specimen – light scattering, refraction and absorption.

All the described effects affect the size of the point spread function of the CLSM, reduce the light intensity in the focal region, and thus reduce the resulting fluorescence signal [2]. As a consequence images captured from deep layers of the specimen may be darker than images from the topmost layers. This fact gives a raise to problems in subsequent image analysis, segmentation and visualization of objects.

A lot of papers devoted to intensity variations correction have been published until now. In computer vision this problem refers to correcting optical flow among images of the scene obtained at two or more different times [3]. A histogram warping based correction has been described in [4], where authors developed a method restricted to the case where a global, spatially invariant, nonlinear, monotonically increasing relationship exists between the intensities of two images. This technique is closely related to works in histogram specification [5].

Another approach lies in the least squares optimization with brightness and contrast being optimized parameters. These techniques are highly sensitive to noise present in images, which is practically always the case of CLSM images. The method in [6] tried to overcome this difficulty by applying an iteratively reweighted least squares method. We experimented with this method, but it gave us erroneous and unstable results even in the case of low-noise optical sections.

In medical imaging there have been published methods for standardization of the grey scale of MRI (magnetic resonance imaging) images [7]. The methods are based on remapping image intensities by matching landmarks found in image histograms.

Some works have dealt with the light attenuation compensation in fluorescence microscopy. Many of them utilize especially modelling the light attenuation due to scattering, absorption and photobleaching by the exponential decay law [6, 8-10].

In this work we propose two methods for compensation of the light attenuation with depth. The first method is an online method, since it works already during the optical sectioning of a specimen and make corrections of image intensities by simple image-

ISSN: 1727-1983

analysis-based tuning of the CLSM hardware. The second method is an offline method used as a post-processing step.

During its development we were inspired especially by methods described in [4] and [7]. We developed a general and automatic approach consisting of two-stages. In the first stage a standard histogram – which maintains relative frequencies of grey levels and improves brightness and contrast – is created from histograms of all optical sections in the stack. In the second stage individual image histograms are warped according to the standard histogram to achieve as uniform as possible contrast and brightness of images within the stack.

In these methods we utilize the fact that all above mentioned light loss contributions, namely wrong staining, light aberrations and photobleaching, combine together to overall light attenuation with depth. It is practically impossible to separate and correct individual light loss components. Therefore, each of our methods utilizes one single parameter comprising and integrating all the light loss components and carry information about the light attenuation. The single parameters used in our methods are the mean intensity value in the case of the online method, and the image histogram in the case of the offline method, respectively.

Both the online and offline methods are required in real practice, since sometimes one has not the investigated specimen at his disposal, but only the scanned data. Then using the offline method is necessary.

The aim of the described methods is to obtain better visualization of data and a possibility to use easier segmentation methods than in the case of original data. For example, a single threshold for segmentation of objects in the whole stack can be applied if specific staining of structures of interest is used.

Main motivation for development of these methods was absence of such algorithms in commercial software packages.

Materials and Methods

Following experiments were performed using a Leica SP2 AOBS confocal laser scanning microscope controlled by a personal computer equipped with the proprietary Leica Confocal Software.

Figure 1 shows a subset of the full series of optical sections of rat skeletal muscle fibres. We depict only every sixth image of the original series here. Note the intensity attenuation and evolving objects in the optical sections in *z*-direction. Excitation wavelength applied was 488 nm and emission wavelengths ranged from 500 to 535 nm. The stack represents a biological specimen characterized by a high portion of background. The upper left image of the figure comes from the topmost layer of the specimen while the bottom right image from the deepest layer. The height of the stack was about 42 μm.

Online method

The used CLSM is controlled by a personal computer equipped with the proprietary Leica Confocal Software containing a Macro Developer giving the user a possibility to develop macros in Visual Basic language to adjust the CLSM hardware.

The main important parameter that can be adjusted during optical sectioning is a gain of a photomultiplier tube. This gain describes amplification of the detected signal of a given channel during scanning in Volts, i.e. the higher the gain, the more amplified detected signal is obtained.

We developed a macro called SCOM (Series Capture Optimization Macro), see Figure 2. In the beginning the user selects a reference image. This means that prior starting the macro, the user has to capture at least one optical section of the investigated specimen. However, better approach is to capture the whole stack of optical sections and then to select the best image from the stack as the reference one.

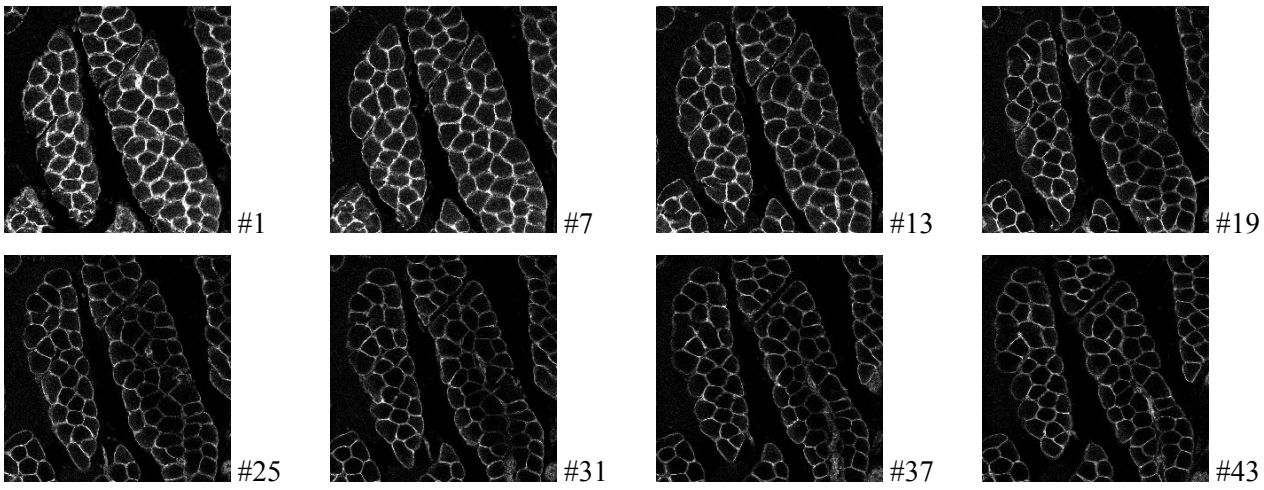

Figure 1: Subset of a series of confocal optical sections of rat skeletal muscle fibers. The distance between sections in the subset is about 6 μm. The numbers depict numerical order of optical sections in the full series.

ISSN: 1727-1983

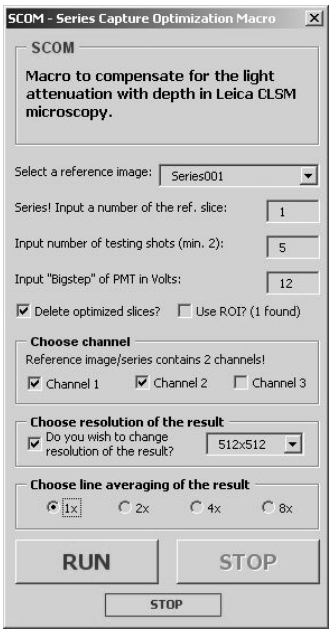

Figure 2: Graphical user interface of the macro SCOM.

Next, the user selects a number of "testing shots". This number represents number of evenly spaced confocal planes to be tested for the mean intensity level of the corresponding optical section. During computation process the macro does not capture and optimize all the optical sections of the specimen, but only this selected subset, see Figure 3. This restriction is performed in order to prevent the bleaching of used fluorochromes in the specimen and to speed up the macro by avoiding the repeated optical sectioning of all images of the specimen, since the sectioning is a relatively slow process.

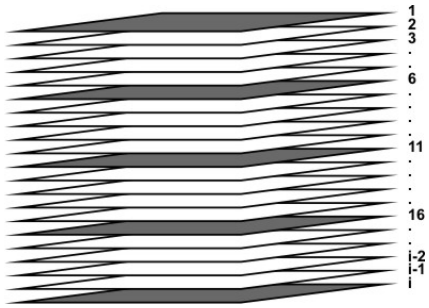

Figure 3: Evenly spaced "testing shots" (dark grey) of a stack of ***i*** confocal planes.

Then the macro performs optimization. It searches for the values of the gain to get optical sections from the selected confocal planes having the same intensity level. As a measure of the intensity level we chose a mean intensity level of an image (MIL). The main advantage of this measure is its independency on pixel positions, since images from different confocal planes of the specimen are not identical.

To get the same value of MIL in the tested planes, the value of the gain is optimized by "*n*-step search". This optimization strategy uses decreasing searching steps to achieve the global minimum of the difference of MIL (DMIL) between the reference section and the investigated section. In our case *n* has value 3. In the first step *n*-step search seeks for the minimum of DMIL using a high step of a gain (e.g. 12 Volts as shown in Figure 2). After finding it, the step in decreased and optimization continues only in the vicinity of the previous result to get the minimum more precise.

After obtaining gain values of all "testing shots", the gain values of all confocal planes are piecewise linearly interpolated and the resulting stack of optical sections is captured. If small or irregular objects are present in the specimen, it is possible to apply the macro only on a selected region of interest. Also, it is possible to select the resolution and line averaging (to remove noise) of the result. The macro can be applied up to three image channels that are optimized consecutively.

Offline method

In the offline method, first, a standard histogram of a stack of images with different intensity levels and contrast is constructed. The aim is to obtain a histogram preserving high contrast of optimally captured optical sections from top layers on one side, and enabling contrast and brightness improvement of dark sections from deep layers on the other side. Then histograms of individual optical sections are warped according to the constructed standard histogram. Thus all images in the stack are forced to have similar contrast and brightness.

Standard Histogram Construction

For construction of the standard histogram we adapted the approach described in [7] which is applied to grey-scale standardization of MRI images. This approach is based on matching landmarks in histograms. We chose the landmarks to be intensities corresponding to the minimum intensity, maximum intensity, and the *n*-th percentiles of the image histogram, $n \in \{10, 20,..., 90\}$. At the beginning the algorithm calculates histograms of all optical sections in the stack and then evaluates landmarks in these histograms.

Further, unlike the original approach that matches the landmarks directly, our algorithm searches for the longest distances between two adjacent landmarks in one histogram, i.e. between the minimum intensity and the tenth percentile or between the tenth percentile and the twentieth percentile, etc. Maximal distances between landmarks are considered in order to preserve maximum image contrast. These distances are searched in all histograms. The maximal distances found are counted up and stretched to cover a greyscale of 256 levels. This scale represents a standard scale according to which a standard histogram is to be computed. The breaks between rescaled maximal distances represent new landmarks of the standard scale.

New intensities of all image pixels of the stack are computed by matching landmarks of the standard scale and landmarks of individual image histograms. Image intensities between landmarks are piece-wise linearly interpolated. The new intensity values are accumulated in the standard histogram. Since frequencies in bins of the standard histogram correspond to the whole stack, they are then adjusted to the size of one optical section.

ISSN: 1727-1983

Histogram Warping

Histogram warping (HSWP) [4] is a method that tries to compensate violations of the constant image brightness assumption. According to this assumption intensities of corresponding points in two or more images of the same scene should be equal. The assumption relates to works in optical flow estimation. HSWP supposes that errors in the constant image brightness assumption can be described by a non-linear monotonically increasing function that uniquely maps intensity values in the first image to intensity values in the second image. HSWP is based on matching one histogram onto another and supposes matching intensities one-to-one (identity), one-to-many (expansion), many-to-one (contraction) or many-to-many (expansion or contraction), see Figure 4.

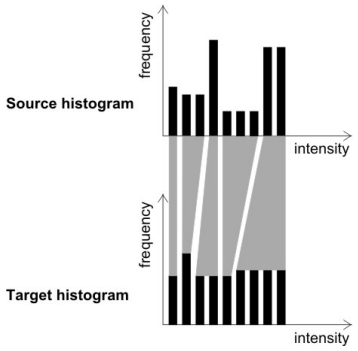

Figure 4: Examples of matching intensities of two histograms; from left to right: 1-1 (identity), 2-1 (contraction), 1-2 (expansion), 3-1 (contraction), 2-4 (many-to-many expansion).

HSWP is based on minimization of a cost function. To specify the cost of a matching, let h_m^α and h_n^β represent the frequency of occurrence in the *m*-th and *n*-th bin of a histogram of the first and second image, respectively. Then the cost of matching intensity I_m^α of the first image with intensity I_n^β of the second image is defined as

$$c_{1,1} = \left| h_m^\alpha - h_n^\beta \right|. \qquad (1)$$

This corresponds to one-to-one mapping. Similarly, the cost of a *k*-to-*l* mapping is expressed by

$$c_{k,l}(m,n) = \left| \sum_{i=0}^{k-1} h_{m-i}^\alpha - \sum_{j=0}^{j-1} h_{n-j}^\beta \right|. \qquad (2)$$

The total cost of a matching is defined recursively as

$$\begin{aligned} &C(0,0) = 0 \\ &C(i,j) = \infty, (i \le 0, j \le 0, (i,j \ne (0,0))) \\ &C(m,n) = \min \begin{cases} C(m-1,n-1) + c_{1,1}(m,n) \\ C(m-1,n-l) + c_{1,l}(m,n), (2 \le l \le N) \\ C(m-k,n-1) + c_{k,l}(m,n), (2 \le k \le M), \end{cases} \end{aligned} \qquad (3)$$

where *M* and *N* represent the maximum allowed contraction and expansion of the histogram, respectively. The total cost is expressed here for one-to-one, one-to-many and many-to-one mappings only, but its extension to high order mappings is straightforward. The cost function (3) is efficiently minimized by dynamic programming.

Results

The online method was implemented within Leica Confocal Software package using Visual Basic 5.0 based Macro Developer, and the offline method as a specialized plug-in of the modular software package Ellipse (Company ViDiTo, Slovakia, www.vidito.com) in C++ language. This package is intended to the processing of biological 2D and 3D images.

First, the specimen was captured under standard conditions, i.e. without using the online correction method. The obtained series of optical sections is shown in Figure 1. Figure 5 depicts their corresponding histograms that are, for clarity, drawn in one image. The decrease of contrast and intensity of the series is evident.

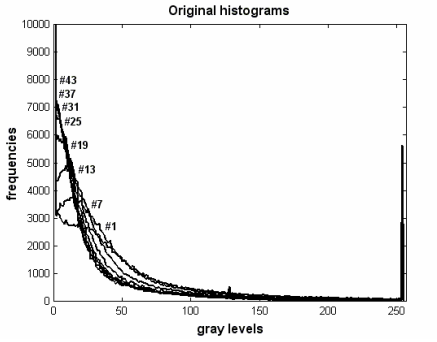

Figure 5: Original histograms of the subsets of series of optical sections of the rat muscle specimen. The numbers in the figure correspond to numerical order of optical sections in the full series.

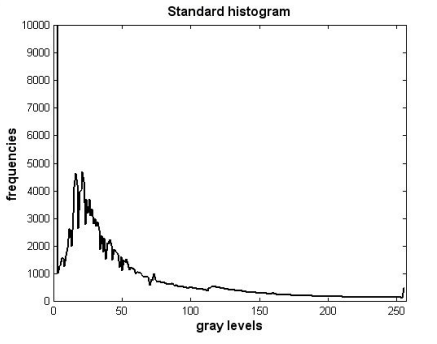

Figure 6: Standard histogram constructed from the full series of the rat muscle specimen.

The obtained stack of optical sections was processed by our offline method. The result is shown in Figure 9. The standard histogram, constructed according to the above mentioned description, is exemplified by Figure 6.

ISSN: 1727-1983

We can see the standard histogram practically spans all peaks from Figure 5, therefore it enhances contrast of individual optical sections, and moves the average brightness towards high intensities. Figure 7 demonstrates resulting warped histograms of the individual optical sections. The shapes of resulting histograms well pursue the shape of the standard histogram, which causes the resulting optical sections have similar brightness and contrast.

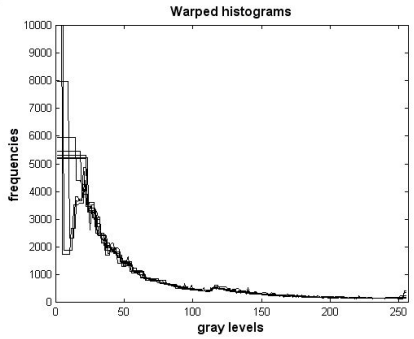

Figure 7: Warped histogram of the subsets of optical sections of the rat muscle specimen.

Second, the specimen was captured by using the online method. As a reference image served the first optical section of the original series. The result is shown in Figure 10.

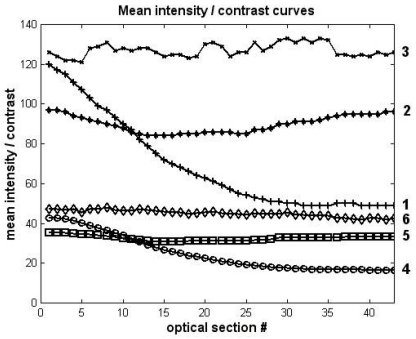

Figure 8: Original contrast (line 1), contrast corrected by the online method (line 2), contrast corrected by the offline method (line 3), original mean intensity (line 4), mean intensity corrected by the online method (line 5), mean intensity corrected by the offline method (line 6).

Figure 8 demonstrates improvement of corrected contrast and brightness of the compensated series over contrast and brightness of original images. We computed image contrast here (noted C_n for the nth optical section) as difference between intensity values corresponding to the 90th percentile $p_{90,n}$ and the 10th percentile $p_{10,n}$ of an image histogram:

$$C_n = p_{90,n} - p_{10,n}\,. \qquad (4)$$

The plot of original contrast /marked 1/ exhibits strong decrease with depth, while both the plots of the online /2/ and offline /3/ corrected contrasts are more constant. The image mean intensity curves are also shown. Again, the plot of mean intensities without correction /4/ shows important brightness decrease, but the plots with online /5/ and offline /6/ corrections become more constant.

Resulting brightness and contrast of the test series corrected by the offline method /lines 3 and 6 in Figure 8/ are even higher than in the case of the online method. This is due to the fact the constructed standard histogram (Figure 6) is broader, i.e. has higher contrast, and its mean intensity is set around higher intensity than the histogram of the reference optical section used in the online method.

Discussion

The goal of this work was to compensate for intensity and contrast loss with depth in confocal microscopy. For this purpose we developed and implemented both an online method and offline method. The online method works during optical sectioning of a specimen while the offline method is used as a post-processing step.

Our experimental results show that the series of sections restored using both the methods are characterized by more constant curves of image contrast and intensity when compared with the original series.

The important advantage of both the described method consists in preserving the information content of optical sections through the whole series. Especially using the online method is highly recommendable, since the improvement of optical sections is generally better when compared with the offline method. But from practical reasons, see below, it is not always possible.

The online method increases time of optical sectioning of a specimen – every confocal plane tested during optimization must be scanned repetitively, and may accelerate the bleaching of used fluorochromes in the specimen. The offline method is computationally fast (cca 2-3 seconds per one optical section using Pentium 4, 2.8 GHz) and does not depend on the microscope. It must be used if one has only captured data and not the specimen available.

Optical sections captured by a CLSM are more or less degraded by noise. In practice it is useful to eliminate this noise by, for example, median filtering. Confocal optical sections are also often multi-channel. In this case, prior to using our algorithm, individual channels must be separated. After intensity correction the channels must be again combined.

According to our preliminary experiments, both the algorithms are general, able to work on various kinds of data sets including sparse stained specimens and specimen with strong contrast and brightness attenuation. Both the methods were successfully tested on more than twenty series of optical sections captured from various specimens. The results confirmed the stability of the algorithms.

ISSN: 1727-1983

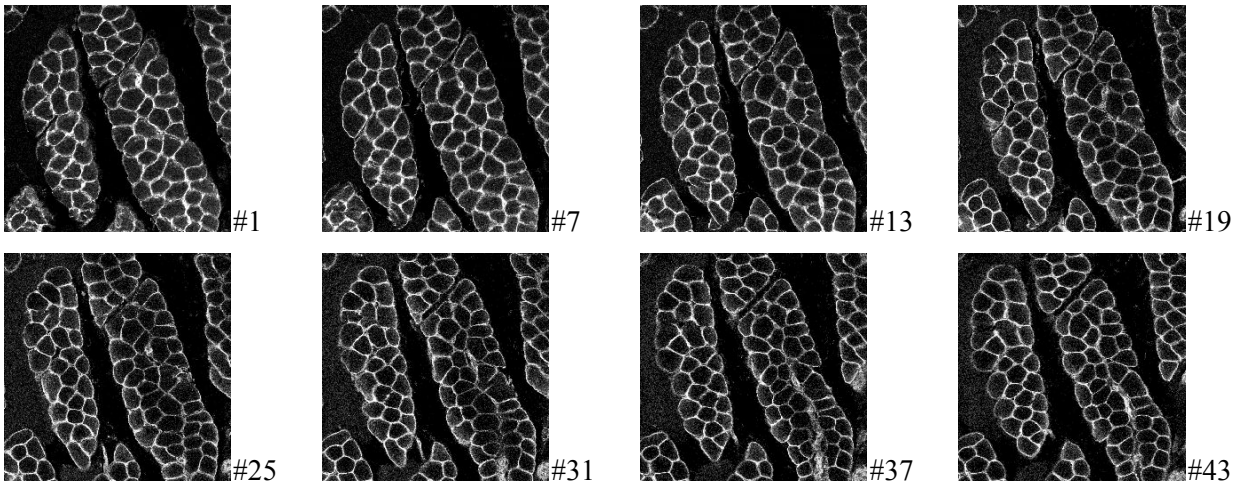

Figure 9: Subset of a series of confocal optical sections of the rat skeletal muscle fibres specimen corrected by the offline method after image acquisition.

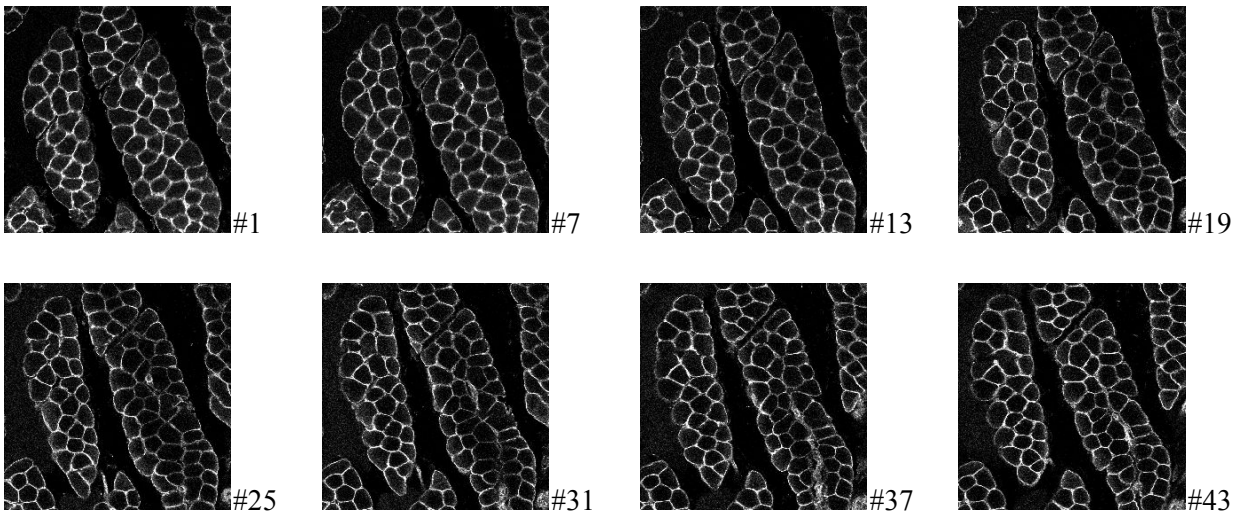

Figure 10: Subset of a series of confocal optical sections of the rat skeletal muscle fibres specimen corrected during image acquisition by the online method.

References

[1]PAWLEY J. (1995): 'Handbook of biological confocal microscopy', (Plenum Press, New York)

[2]DIASPRO A., editor (2002): 'Confocal and Two-Photon Microscopy, Foundation, Applications, and Advances', (Wiley-Liss, New York)

[3]NEGAHDARIPOUR P. (1998): 'Revised definition of optical flow: integration of radiometric and geometric clues for dynamic scene analysis', *IEEE Trans. Pattern Anal. Mach. Intell.*, **20**, pp. 961-979

[4]COX I. J., ROY S., HINGORANI S. L. (1995): 'Dynamic Histogram Warping of Image Pairs for Constant Image Brightness', Proc. of IEEE Image Processing, p. 366-369

[5]GONZALES R. C., WOODS R. E. (1993): 'Digital Image Processing', (Addison-Wesley, New York)

[6]KERVRANN C., LEGLAND D., PARDINI L. (2004): 'Robust incremental compensation of the light attenuation with depth in 3D fluorescence microscopy', *J. Microsc.*, **215**, pp. 297-314

[7]NYÚL L. G., UDUPA J. K., ZHANG X. (2000): 'New Variants of a Method of MRI Scale Standardization', *IEEE Trans. Med. Imaging*, **19**, pp. 143-150

[8]GHAUHARALI R. I., BRAKENHOFF G. J. (2000): 'Fluorescence photobleaching-based image standardization for fluorescence microscopy', *J. Microsc.*, **198**, pp. 88-100

[9]MARKHAM J., CONCHELLO J. A. (2001): 'Artefacts in restored images due to intensity loss in three-dimensional fluorescence microscopy', *J. Microsc.*, **204**, pp. 93-98

[10]SUN Y., BARTEK R., ROBINSON J. P., (2004): 'Adaptive image-processing technique and effective visualization of confocal microscopy images', *Microsc Res Tech*, **64**, pp. 156-163

ISSN: 1727-1983